Ionization penalty in nonlinear optical bioimaging

A. A. Voronin and A. M. Zheltikov
Physics Department, International Laser Center, M. V. Lomonosov Moscow State University, Vorob'evy gory, Moscow 119992, Russia
(Received 20 October 2009; revised manuscript received 2 February 2010; published 17 May 2010)

The noninvasiveness of nonlinear optical imaging techniques is quantified in terms of the number of free electron generated in the laser-tissue interaction region per photon emitted into the nonlinear optical signal. For a broad variety of biomarker dyes and bioactivity reporter proteins, this ratio is shown to approach a critical value of unity for field intensities above 1 $\mathrm{TW/cm^2}$. Closed-form analytical expressions for the ionization penalty function and the critical pulse repetition rate are derived for few-cycle laser pulses.

DOI: 10.1103/PhysRevE.81.051918 PACS number(s): 87.64.−t, 33.80.Rv

I. INTRODUCTION

Nonlinear optics provides a broad variety of powerful tools for microspectroscopy and imaging of biological tissues [1–3] and offers attractive solutions for the diagnostics of anomalies in biological objects, laser therapy, and high-precision surgery [4,5]. Multiphoton absorption (MPA) is a backbone of a broad variety of bioimaging techniques and biomedical strategies, including high-resolution microscopy [1–3], photodynamic therapy [4], drug-delivery monitoring and drug activation [6]. Coherent anti-Stokes Raman scattering [7,8] and stimulated Raman scattering [9] find growing applications for chemically selective imaging, visualization of processes inside cells, endoscopy, and brain imaging. Stimulated-emission depletion and related techniques [10,11] break the records of spatial resolution, leading us to rethinking and redefining the fundamental limitations on spatial resolution in optical microscopy and imaging.

With the intensity of a nonlinear optical signal resulting from an N-photon process scaling as I^N with the field intensity I, high I values are necessary for the fast and reliable detection of nonlinear signal in nonlinear optical imaging schemes. In view of this scaling, laser intensities are often chosen for nonlinear imaging in such a way as to avoid visible laser-induced damage of a sample in the focus of the laser beam. With such a strategy, however, it is difficult, if possible at all, to understand and control the degree of modifications induced by laser pulses in biotissues, as well as to avoid unwanted cumulative effects caused by the action of laser pulses on soft matter in the regime of high-repetition rates. This raises serious concerns about the noninvasiveness of nonlinear optical techniques, calling for in-depth quantitative studies of the interaction of high-intensity, high-repetition-rate laser pulses with soft matter.

In this paper, we will demonstrate that the noninvasiveness of nonlinear optical imaging techniques is quantified in terms of the number of free electron generated in the laser-tissue interaction region per photon emitted into the nonlinear optical signal. We will also derive closed-form analytical expressions for the ionization penalty function and the critical repetition rate of laser pulses above which free electrons are accumulated in a laser-irradiated region, leading to an optical damage of a biotissue. Predictions of these formulas will be compared with numerical simulations based on a more accurate model of water ionization, which includes photoionization and avalanche ionization, as well as carrier diffusion and recombination.

II. ANALYTICAL TREATMENT

We start with a simple approximate analysis of ionization-induced buildup of electron density in a soft-matter medium irradiated by ultrashort laser pulses in a typical MPA imaging experiment. The density of free electrons generated by a laser pulse in the regime of multiphoton ionization is given by

$$\rho(t) = \int_{-\infty}^{t} W_{ph}(\theta) d\theta = \rho_0 \sigma_N \int_{-\infty}^{t} \left[\frac{I(\theta)}{\hbar \omega} \right]^N d\theta, \qquad (1)$$

where $W_{ph}(\theta) = \rho_0 \sigma_N \left[\frac{I(\theta)}{\hbar\omega}\right]^N$ is the rate of N-photon ionization, ρ_0 is the steady-state electron density in the ground state, ω is frequency, σ_N is the cross section of N-photon ionization, and $I(\theta)$ is the temporal envelope of the field intensity.

The cross section of multiphoton ionization σ_N will be defined in this work by applying a $\rho_0 \sigma_N (I_0/\hbar\omega)^N$ fit to the photoionization rate W_{ph} calculated as a function of the field intensity by using the Keldysh model of ionization [12] in a direct-gap semiconductor with a band gap $U_0 \approx 6.5$ eV. In reality, ionization of water is, of course, much more complicated than ionization of a direct-gap semiconductor. It involves a variety of competing ionization and dissociation mechanisms and scenarios depending on the laser frequency and the way solvating water molecules are organized about charge [13–15]. While the band gap of liquid water has been estimated as 6.9 eV, direct vertical transitions from the valence-band edge to the conduction-band edge are known to have a very low probability. On the other hand, solvated electrons can be generated in water by UV radiation with photon energies slightly above 6 eV [16], with the most probable mechanism behind this photoionization process being dissociative proton-coupled electron transfer to a preexisting trap [17]. Despite the complexity of ultrafast dissociative and ionization dynamics of water, a compact closed-form model of water photoionization based on the Keldysh formalism with an effective band gap $U_0 \approx 6.5$ eV has been shown to provide a good fit for the density of electrons in liquid water measured as a function of the laser intensity [18–20] and to allow an adequate description of the evolution of ultrashort high-intensity laser pulses in water [21–26]. In what follows, we apply this phenomenological model of

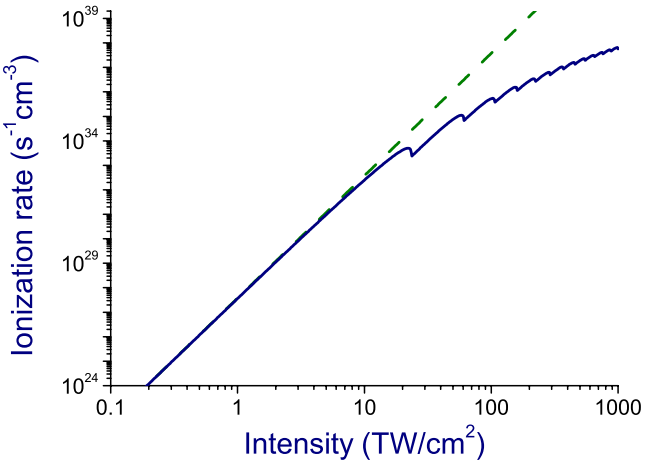

FIG. 1. (Color online) Ionization rate calculated as a function of the laser field intensity for a water-type medium with a band gap $U_0 \approx 6.5$ eV irradiated by laser pulses with a central wave length $\lambda = 800$ nm. Calculations are performed with the use of the Keldysh formalism (solid line) and the $\rho_0 \sigma_5 (I_0/\hbar\omega)^5$ fit with $\sigma_5 \approx 5.22 \cdot 10^{-149}$ cm^{10} s^4 photon^{-4}, $\rho_0 = 6.7 \cdot 10^{22}$ cm^{-3} (dashed curve).

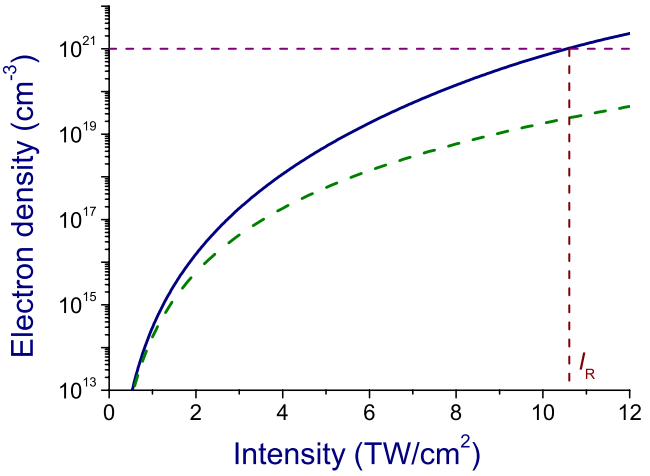

FIG. 2. (Color online) The electron density in the wake of the laser pulse as a function of the laser field intensity for $U_0 \approx 6.5$ eV, $\lambda = 800$ nm, and the FWHM pulse width $\tau_{FWHM} \approx 1.665\tau_p = 100$ fs. Calculations are performed through a numerical solution of Eq. (10) (solid line) and by using the explicit result of Eq. (2).

photoionization to derive closed-form analytical expressions and quantitative estimates for the ionization penalty and the critical pulse repetition rate in nonlinear optical bioimaging using ultrashort laser pulses.

For a Gaussian intensity envelope, $I(\theta) = I_0 \exp[-(\theta/\tau_p)^2]$, τ_p being the pulse width, Eq. (1) yields the following expression for the electron density in the wake of the laser pulse:

$$\rho = \rho_0 \sigma_N \left[\frac{I_0}{\hbar\omega}\right]^N \int_{-\infty}^{\infty} \exp\left(-N\frac{\theta^2}{\tau_p^2}\right) d\theta = \left(\frac{\pi}{N}\right)^{1/2} \rho_0 \sigma_N \left[\frac{I_0}{\hbar\omega}\right]^N \tau_p. \quad (2)$$

For a water-type medium with a band gap $U_0 \approx 6.5$ eV irradiated by laser pulses with a central wavelength $\lambda = 800$ nm (typical of Ti: sapphire lasers), the number of photons required for photoionization is $N = 5$. The five-photon ionization cross section σ_5 can be found by applying the $\rho_0 \sigma_5 (I_0/\hbar\omega)^5$ fit (the dashed curve in Fig. 1) to the photoionization rate W_{ph} calculated as a function of the field intensity by using the Keldysh formalism [12] (the solid curve in Fig. 1). This procedure yields $\sigma_5 \approx 5.22 \cdot 10^{-149}$ cm^{10} s^4 photon^{-4} at $\lambda = 800$ nm for a dielectric material with $U_0 \approx 6.5$ eV, $\rho_0 = 6.7 \cdot 10^{22}$ cm^{-3}.

With the laser field intensity increasing from 1 to 10 TW/cm^2, the electron-density induced in a water-type soft-matter medium through five-photon ionization in the wake of a laser pulse ranges from 10^{14} to 10^{19} cm^{-3} (the dashed line in Fig. 2 and solid line 1 in Fig. 3). As ρ approaches the critical electron density $\rho_c = m\omega^2(4\pi)^{-1}e^{-2}$, where m and e are the electron mass and charge, respectively, and ω is the radiation frequency, the medium becomes strongly absorbing at the frequency ω. The laser damage of a condensed material typically occurs at electron density levels somewhat lower than ρ_c [27–29]. Throughout this work, the damage threshold intensity for radiation with $\lambda = 800$ nm will be understood (with a certain degree of arbitrariness) as the field intensity that generates an electron density $\rho_d = 10^{21}$ cm^{-3} in the wake of the laser pulse. This definition is consistent with the earlier work on the laser damage of condensed-phase materials [27–29]. As shown in Fig. 2, with $U_0 \approx 6.5$ eV, $\lambda = 800$ nm, and the full width at half maximum (FWHM) pulse width $\tau_{FWHM} \approx 1.665\tau_p = 100$ fs, the electron density ρ_d (shown by the horizontal dashed line in Fig. 2) is generated by a laser pulse with $I_R \approx 10.5$ TW/cm^2. The damage threshold intensity is shown by the vertical dashed line in Fig. 2.

We now consider the luminescent response of a molecular system excited through M-photon absorption. The number of photons emitted in this luminescent signal is given by

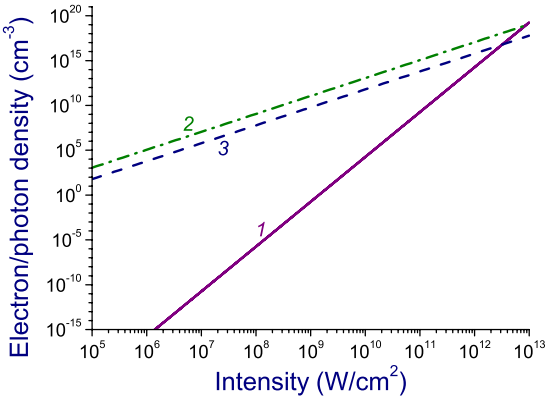

FIG. 3. (Color online) The density of free electrons in the wake of a laser pulse (1) and the density of photons emitted through two-photon-excited luminescence (2, 3) in a 0.1-mM solution of (2) Rhodamine B ($\sigma_{TPA} \approx 150$ GM, $\eta = 1$) and (3) wild-type green fluorescent protein ($\sigma_{TPA} \approx 6.5$ GM, $\eta = 1$) as a function of the field intensity for $U_0 \approx 6.5$ eV, $\lambda = 800$ nm, and $\tau_{FWHM} = 100$ fs.

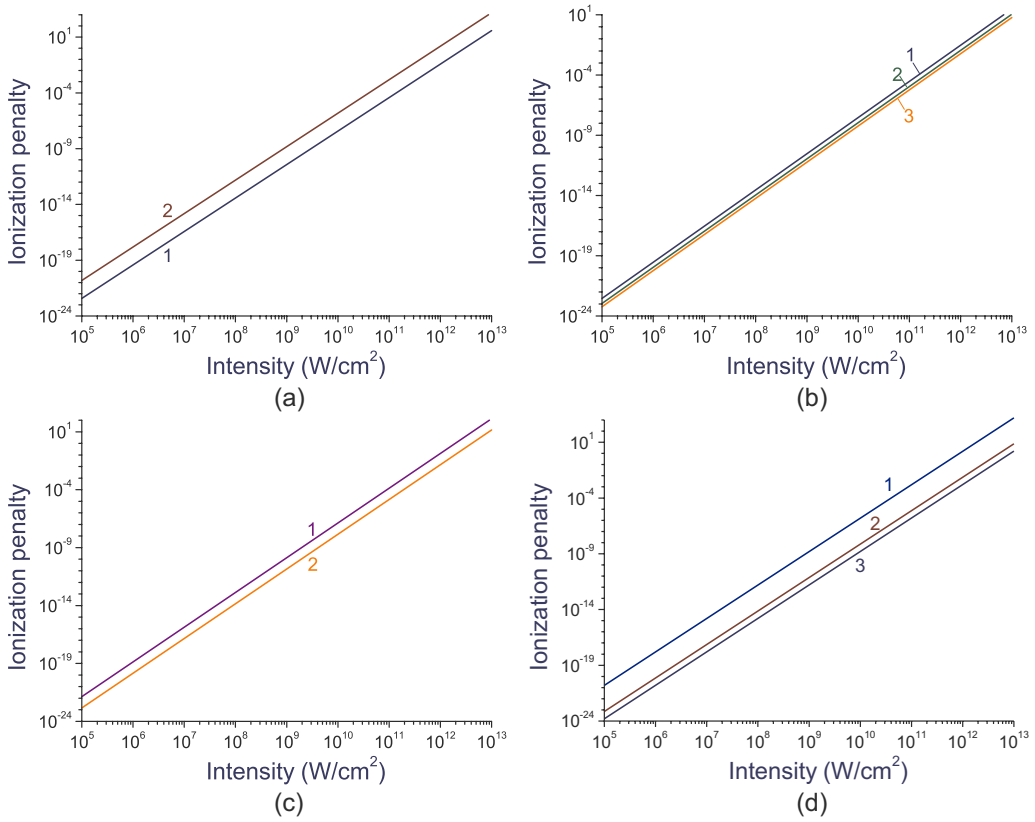

FIG. 4. (Color online) Ionization penalty function $\xi=\rho/n_{ph}$ calculated for a 0.1-mM solution of various biomarker dyes and bioactivity reporter proteins used in bioimaging: (a) wild-type GFP, $\sigma_{\mathrm{TPA}}\approx 6.5$ GM (1); Indo-1 free, $\sigma_{\mathrm{TPA}}\approx 0.16$ GM (2); (b) Fura-2 free and Fluo-3 with Ca^{2+}, $\sigma_{\mathrm{TPA}}\approx 8.3$ GM (1); calcium green-1 with Ca^{2+}, $\sigma_{\mathrm{TPA}}\approx 22$ GM (2); calcium orange with Ca^{2+}, $\sigma_{\mathrm{TPA}}\approx 42$ GM (3); (c) Bodipy and Lucifer yellow, $\sigma_{\mathrm{TPA}}\approx 1.8$ GM (1), Coumarin 307, $\sigma_{\mathrm{TPA}}\approx 17$ GM (2); (d) DiI, $\sigma_{\mathrm{TPA}}\approx 0.15$ GM (1), fluorescein, $\sigma_{\mathrm{TPA}}\approx 33$ GM (2); Rhodamine B, $\sigma_{\mathrm{TPA}}\approx 150$ GM (3); $U_0\approx 6.5$ eV, $\lambda=800$ nm.

$$n_{ph}=n_0\eta\sigma_{MPA}\int\left[\frac{I(\theta)}{\hbar\omega}\right]^M d\theta, \tag{3}$$

where n_0 is the initial concentration of luminescent species, σ_{MPA} is the cross section of M-photon absorption, and η is the quantum yield of fluorescence.

Integration for a Gaussian pulse then yields

$$n_{ph}=n_0\eta\sigma_{MPA}\left(\frac{\pi}{M}\right)^{1/2}\left(\frac{I_0}{\hbar\omega}\right)^M\tau_p. \tag{4}$$

In a particular case of two-photon absorption-excited luminescence (TPL), Eq. (4) reduces to

$$n_{ph}=n_0\eta\sigma_{TPA}\left(\frac{\pi}{2}\right)^{1/2}\left(\frac{I_0}{\hbar\omega}\right)^2\tau_p, \tag{5}$$

where σ_{TPA} is the cross section of two-photon absorption (TPA).

In Fig. 3, we plot the TPL photon density calculated as a function of the field intensity I_0 for dye and biomarker molecules widely used in bioimaging, such as Rhodamine B ($\sigma_{\mathrm{TPA}}\approx 150$ GM$=1.5\cdot 10^{-48}$ cm^4 s/photon, dashed line 2), and wild-type green fluorescent protein (GFP) ($\sigma_{\mathrm{TPA}}\approx 6.5$ GM$=6.5\cdot 10^{-50}$ cm^4 s/photon, dashed line 3). Due to the nonlinear nature of TPL, the number of TPL photons n_{ph}, as can be seen from Eq. (4) and Fig. 3, scales as $n_{ph}\propto I_0^2$ with the field intensity. This increase in n_{ph} is, however, not penalty free, as the density of free-electrons ρ increases even faster, $\rho\propto I_0^5$ [Eq. (2) and Fig. 3], because of the higher nonlinearity of the multiphoton ionization process. As a result, above a certain critical field intensity I_c, each TPL photon is produced with a penalty of more than one free electron generated through multiphoton ionization. Based on the calculations presented in Fig. 3, this critical intensity is estimated as 3 TW/cm^2 for wild-type GFP and 9 TW/cm^2 for Rhodamine B.

This leads us to defining an ionization penalty function for MPA imaging as a ratio of the electron density in the wake of a laser pulse to the number of photons induced through MPA, $\xi=\rho/n_{ph}$. With approximations of Eqs. (1)–(4), we find

$$\xi=\left(\frac{M}{N}\right)^{1/2}\frac{\rho_0\sigma_N}{\sigma_{MPA}n_0\eta}\left(\frac{I_0}{\hbar\omega}\right)^{N-M}. \tag{6}$$

In the case of TPA imaging ($M=2$), the ionization penalty function is given by

$$\xi=\left(\frac{2}{N}\right)^{1/2}\frac{\rho_0\sigma_N}{\sigma_{TPA}n_0\eta}\left(\frac{I_0}{\hbar\omega}\right)^{N-2}. \tag{7}$$

In Figs. 4(a)–4(d), we plot the penalty function $\xi=\rho/n_{ph}$ calculated for various biomarker dyes and bioactivity re-

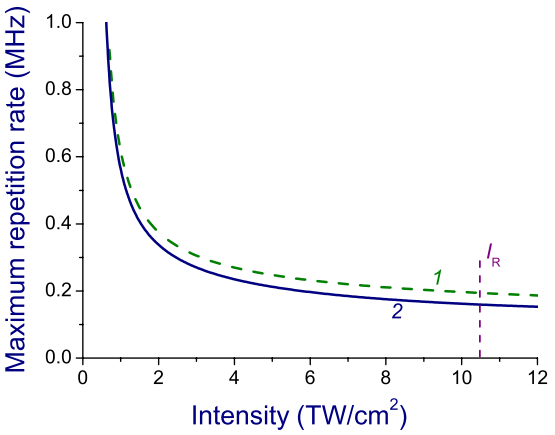

FIG. 5. (Color online) The critical repetition rate f_c calculated as a function of the laser intensity for a water-type medium with $U_0 \approx 6.5$ eV, $\sigma_5 \approx 5.22 \cdot 10^{-149}$ cm^{10} s^4 photon^{-4}, $\rho_0 = 6.7 \cdot 10^{22}$ cm^{-3}, and $\tau_h = 300$ ns irradiated by laser pulses with $\lambda = 800$ nm and $\tau_{FWHM} = 100$ fs: (1) only photoionization is included, (2) both photoionization and avalanche ionization are included.

porter proteins used in bioimaging [30–33]. Results of these calculations demonstrate that, for a broad variety of biomarker dyes and bioactivity reporter proteins, the ratio $\xi = \rho / n_{ph}$ approaches a critical value of unity for peak field intensities above 1 TW/cm^2. Accumulation of free electrons and ionization of water molecules in soft-matter media tend to initiate several unwanted processes in biotissues [19], including the formation of reactive oxygen species [20], causing the death of cells, and DNA-strand breaking by low-energy electrons due to the rapid decay of transient molecular resonances localized on DNA constituents [34].

At high repetition rates, free electrons generated by individual laser pulses can accumulate in a biotissue from pulse to pulse because of a long lifetime τ_h of hydrated electrons in water ($\tau_h \approx 300$ ns [20]). The critical repetition rate f_c above which electrons start to accumulate in a soft-matter medium can be found from the condition

$$V\rho \exp\left(-\frac{1}{f_c \tau_h}\right) = 1, \tag{8}$$

where V is the volume of a laser-irradiated biotissue. Physically, Eq. (8) implies that the electron density generated by the ith laser pulse is such that the number of free electrons remaining in the tissue by the time when it is irradiated by the $(i+1)$th pulse is equal to 1.

For a Gaussian pulse, Eqs. (2) and (8) give

$$I_f = \left(\frac{N}{\pi}\right)^{\frac{1}{2N}} \hbar\omega (V\rho_0 \sigma_N \tau_p)^{-\frac{1}{N}} \exp\left(\frac{1}{fN\tau_h}\right). \tag{9}$$

Figure 5 displays the critical repetition rate f_c calculated as a function of the laser intensity for a water-type medium with $U_0 \approx 6.5$ eV (corresponding to $N=5$), $\sigma_5 \approx 5.22 \cdot 10^{-149}$ cm^{10} s^4 photon^{-4}, $\rho_0 = 6.7 \cdot 10^{22}$ cm^{-3}, and $\tau_h = 300$ ns irradiated by laser pulses with $\lambda = 800$ nm and $\tau_{FWHM} = 100$ fs. The interaction region was assumed to have a shape of an ellipsoid with the volume $V = 4\pi r_0^2 l_0 / 3$ defined by semiaxes $r_0 = 1.22\lambda/(2n_r)$ and $l_0 = \pi n_r \lambda^{-1} r_0^2$, n_r being the refractive index of the soft-matter material, mimicking typical diffraction-limited focusing in an imaging experiment. These calculations show that, with a laser intensity of 1 TW/cm^2, accumulation of free electrons limits the pulse repetition rate at the level of approximately 0.6 MHz.

III. NUMERICAL MODEL

We now compare our predictions based on approximate expressions of Eqs. (1)–(9) with the results of numerical analysis of ionization effects in a more accurate model of laser−soft-matter interaction [18,20] including multiphoton and avalanche ionization, as well as carrier diffusion and recombination. The evolution of the electron density in this model is governed by the equation

$$\frac{\partial \rho}{\partial t} = W_{ph} + \left(\frac{\partial \rho}{\partial t}\right)_a + \left(\frac{\partial \rho}{\partial t}\right)_d + \left(\frac{\partial \rho}{\partial t}\right)_r, \tag{10}$$

which includes the terms accounting for photoionization, avalanche ionization, diffusion of electrons from the interaction regime, and recombination of free carriers.

Avalanche ionization takes place when free electrons produced in a medium due to photoionization acquire an energy from the electromagnetic field through the inverse bremsstrahlung process that is sufficient to generate more free electrons by impact ionization [35]. Here, we use a standard assumption [18,20] that any electron that acquires a certain threshold energy will inevitably generate a new free electron. The threshold energy for this $(e,2e)$ process is set equal to $3U_{\text{eff}}/2$, where $U_{\text{eff}} = 2\pi^{-1} U_0 E(\Phi) \Gamma^{-1/2}$ is the effective ionization potential, $\Phi = (1+\gamma^2)^{-1}$, $\Gamma = \gamma^2 (1+\gamma^2)^{-1}$, $\gamma = \omega_0 (m_e U_0)^{1/2} (eE_0)^{-1}$ is the Keldysh parameter, E_0 is the amplitude of the electric field, m_e is the effective mass of a quasifree electron, $E(\Phi)$ is the second-kind elliptical integral. Then, following Vogel *et al.* [20], we can represent the avalanche ionization term as

$$\left(\frac{\partial \rho}{\partial t}\right)_a = \begin{cases} \dfrac{\psi\rho}{1+\psi\delta_r}, & \rho V \geq 0.5 \\ 0, & \rho V < 0.5 \end{cases}. \tag{11}$$

Here, $\delta_r = n_U \tau_D$, n_U is the number of absorbed photons required to gain the energy $3U_{\text{eff}}/2$, τ_D is the electron momentum transfer time,

$$\psi = \frac{2}{3}\frac{\sigma_D}{U_{\text{eff}}} - \frac{\tau_D}{1+\omega^2\tau_D^2}\frac{m_e\omega^2}{\mu}, \tag{12}$$

$\sigma_D = e^2 \tau_D (c n_r \varepsilon_0 m_e)^{-1} (1+\omega^2\tau_D^2)^{-1}$ is the Drude-type inverse bremsstrahlung cross section, μ is the mass of biotissue (water) molecules.

The diffusion of electrons out of the interaction region is included [18,20] through the term

$$\left(\frac{\partial \rho}{\partial t}\right)_d = -\frac{\rho}{\theta_d}, \tag{13}$$

where

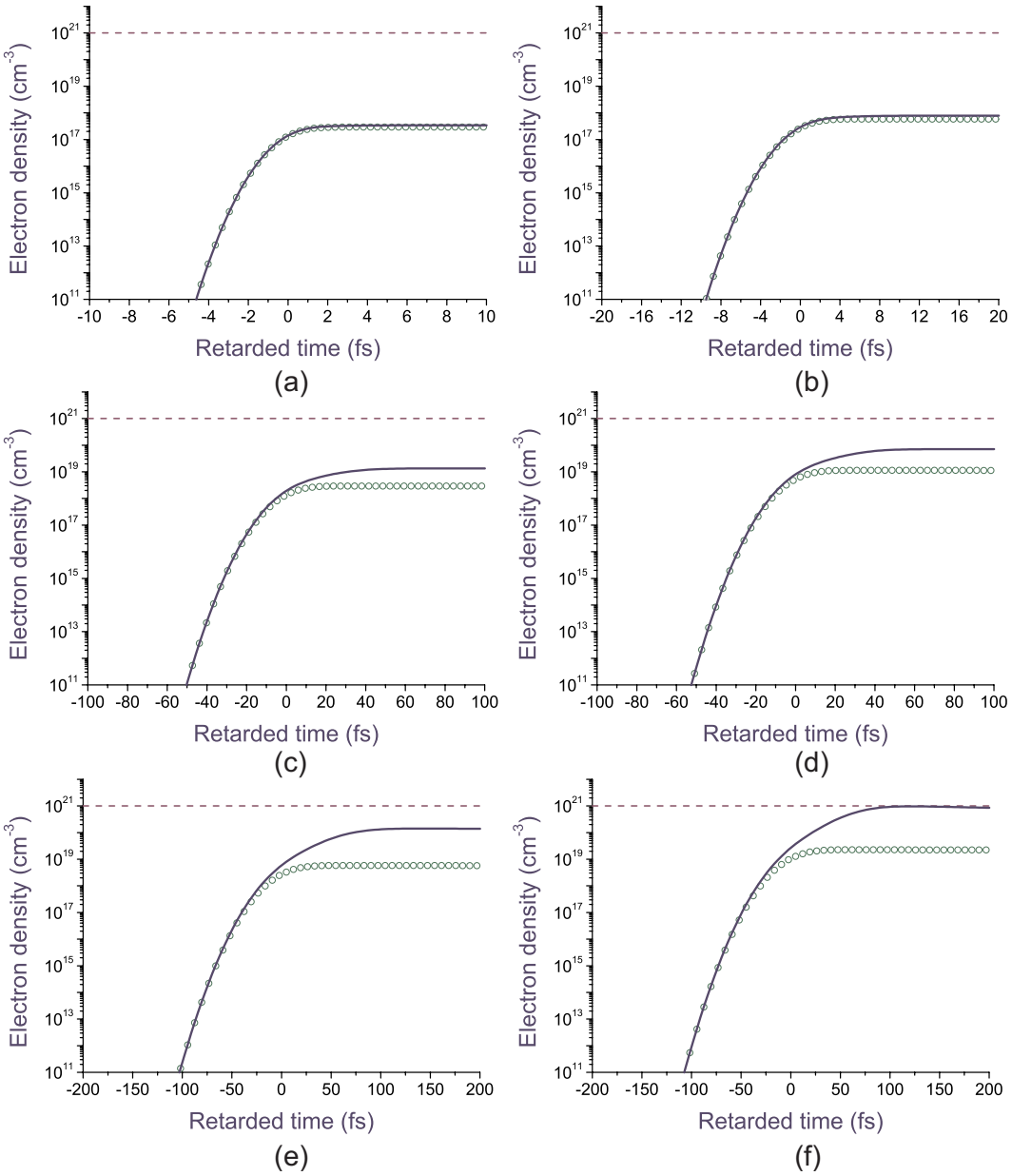

FIG. 6. (Color online) Temporal profiles of the electron density calculated by using Eq. (10) with (solid curves) and without (open circles) inclusion of the avalanche ionization term for different pulse widths and field intensities: (a) $I_0=8$ TW/cm^2, $\tau_{FWHM}=5$ fs; (b) $I_0=8$ TW/cm^2, $\tau_{FWHM}=10$ fs; (c) $I_0=8$ TW/cm^2, $\tau_{FWHM}=50$ fs; (d) $I_0=10.5$ TW/cm^2, $\tau_{FWHM}=50$ fs; (e) $I_0=8$ TW/cm^2, $\tau_{FWHM}=100$ fs; and (f) $I_0=10.5$ TW/cm^2, $\tau_{FWHM}=100$ fs; $U_0\approx 6.5$ eV, $\lambda=800$ nm.

$$\theta_d = \frac{6m_e}{5U_{\text{eff}}\tau_D}\left(\frac{6}{r_0^2}+\frac{2}{l_0^2}\right)^{-1}, \tag{14}$$

is the diffusion time.

Finally, the recombination term is written as [18,20]

$$\left(\frac{\partial\rho}{\partial t}\right)_r = -\zeta_r\rho^2, \tag{15}$$

where ζ_r is a constant, which can be often defined phenomenologically.

For a water-type medium, $U_0\approx 6.5$ eV, $\tau_D\approx 1.7$ fs, and $n_U=7$ [18,20]. With $\lambda=800$ nm, the diffusion time defined by Eq. (14) is estimated as $\theta_d\approx 20$ ps, suggesting that diffusion effects are negligible for the studied regime. A standard estimate of the constant ζ_r for water is $\zeta_r\approx 2\cdot 10^{-9}$ cm^3 s^{-1}. With an electron density on the order of 10^{20} cm^{-3} such a value of ζ_r corresponds to an effective recombination time $\theta_r=(\rho\xi_r)^{-1}\approx 5$ ps. Thus, on the femtosecond time scale, only photoionization and avalanche ionization significantly contribute to the generation of free electrons in a water-type soft-matter medium.

In Figs. 6(a)–6(f), we compare temporal profiles of the electron density calculated by using Eq. (10) with (solid curves) and without (open circles) inclusion of the avalanche ionization term for different pulse widths and field intensities. For few-cycle pulse widths, the contribution of

avalanche ionization to the generation of free electrons is negligible [Figs. 6(a) and 6(b)] because the time interval when the field is applied is too short for the avalanche to build up. In this regime, free-electron generation is dominated by photoionization, and temporal profiles of the electron intensity calculated with and without the avalanche term in Eq. (10) are indistinguishable on the scale of Figs. 6(a) and 6(b). For longer pulse widths, however, a careful inclusion of the avalanche ionization is critical for the quantitative analysis of carrier generation and ionization penalty in laser −soft-matter interactions [Figs. 6(c)–6(f)]. In particular, with $I_0=10.5$ TW/cm^2 and $\tau_{FWHM}=100$ fs, photoionization alone would provide an electron density of $2.3\cdot10^{19}$ cm^{-3} in the wake of the laser pulse [the dashed curve in Fig. 2 and open circles in Fig. 6(f)], which is a factor of 43 lower than the radiation damage electron density ρ_d. When both photoionization and avalanche ionization are included in the model [the solid curves in Figs. 2 and 6(f)], the electron density induced in the medium in the wake of the laser pulse with the same peak intensity and pulse width is exactly equal to ρ_d. With shorter pulse widths, a peak intensity of 10.5 TW/cm^2 can be applied without causing a damage of the medium [Fig. 6(d)], as the time interval within which the field is applied is too short for the generation of the electron density equal to ρ_d. For sufficiently long pulse widths ($\tau_{FWHM}=100$ fs in Fig. 5), the avalanche ionization also lowers the critical repetition rate f_c above which electrons start to accumulate in a soft-matter medium (cf. solid and dashed curves in Fig. 5), eventually leading to optical damage.

IV. CONCLUSION

We have demonstrated in this paper that the noninvasiveness of nonlinear optical imaging techniques can be quantified in terms of the number of free electron generated in the laser-tissue interaction region per photon emitted into the nonlinear optical signal. For a broad variety of biomarker dyes and bioactivity reporter proteins, this ratio is shown to approach a critical value of unity for field intensities above 1 TW/cm^2. We have also derived closed-form approximate analytical expressions for the ionization penalty function and the critical repetition rate of laser pulses above which free electrons are accumulated in a laser-irradiated region, leading to an optical damage of a biotissue. These analytical formulas are shown to be highly accurate in the regime of few-cycle pulse widths, when free-electron generation is dominated by photoionization, while the contribution of avalanche ionization is negligible.

ACKNOWLEDGMENTS

This work was partially supported by the Russian Federal Science and Technology Program, the 7th Framework Program of the European Union, and International Science and Technology Center. A.A.V. also acknowledges the support of his work by the Russian Foundation for Basic Research (Projects No. 08-02-91756, No. 09-02-12359, and No. 09-02-12373).

[1] W. Denk, J. H. Strickler, and W. W. Webb, Science **248**, 73 (1990).
[2] W. R. Zipfel, R. M. Williams, and W. W. Webb, Nat. Biotechnol. **21**, 1369 (2003).
[3] F. Helmchen and W. Denk, Nat. Methods **2**, 932 (2005).
[4] J. D. Bhawalkar, N. D. Kumar, C.-F. Zhao, and P. N. Prasad, J. Clin. Laser Med. Surg. **15**, 201 (1997).
[5] U. K. Tirlapur and K. König, Nature (London) **418**, 290 (2002).
[6] W. G. Fisher, W. P. Partridge, Jr., C. Dees, and E. A. Wachter, Photochem. Photobiol. **66**, 141 (1997).
[7] A. M. Zheltikov, J. Raman Spectrosc. **38**, 1052 (2007).
[8] J.-X. Cheng and X. S. Xie, J. Phys. Chem. B **108**, 827 (2004).
[9] C. W. Freudiger, W. Min, B. G. Saar, S. Lu, G. R. Holtom, C. He, J. C. Tsai, J. X. Kang, and X. Sunney Xie, Science **322**, 1857 (2008).
[10] S. W. Hell, Nat. Biotechnol. **21**, 1347 (2003).
[11] S. W. Hell, Nat. Methods **6**, 24 (2009).
[12] L. V. Keldysh, Zh. Eksp. Teor. Fiz. **47**, 1945 (1964) [Sov. Phys. JETP **20**, 1307 (1965)].
[13] J. V. Coe, A. D. Earhart, M. H. Cohen, G. J. Hoffman, H. W. Sarkas, and K. H. Bowen, J. Chem. Phys. **107**, 6023 (1997).
[14] V. Poterya, M. Farnik, M. Oncak, and P. Slavicek, Phys. Chem. Chem. Phys. **10**, 4835 (2008).
[15] C. G. Elles, A. E. Jailaubekov, R. A. Crowell, and S. E. Bradforth, J. Chem. Phys. **125**, 044515 (2006).
[16] J. W. Boyle, J. A. Ghormley, C. J. Hochanadel, and J. F. Riley, J. Phys. Chem. **73**, 2886 (1969).
[17] D. M. Bartels and R. A. Crowell, J. Phys. Chem. A **104**, 3349 (2000).
[18] P. K. Kennedy, IEEE J. Quantum Electron. **31**, 2241 (1995).
[19] A. Vogel and V. Venugopalan, Chem. Rev. **103**, 577 (2003).
[20] A. Vogel, J. Noack, G. Hüttman, and G. Paltauf, Appl. Phys. B: Lasers Opt. **81**, 1015 (2005).
[21] A. Dubietis, E. Gaizauskas, G. Tamosauskas, and P. Di Trapani, Phys. Rev. Lett. **92**, 253903 (2004).
[22] M. Kolesik, E. M. Wright, and J. V. Moloney, Phys. Rev. Lett. **92**, 253901 (2004).
[23] A. Dubietis, A. Couairon, E. Kučinskas, G. Tamošauskas, E. Gaižauskas, D. Faccio, and P. Di Trapani, Appl. Phys. B: Lasers Opt. **84**, 439 (2006).
[24] S. Minardi, A. Gopal, M. Tatarakis, A. Couairon, G. Tamošauskas, R. Piskarskas, A. Dubietis, and P. Di Trapani, Opt. Lett. **33**, 86 (2008).
[25] S. Minardi, A. Gopal, A. Couairon, G. Tamoašuskas, R. Piskarskas, A. Dubietis, and P. Di Trapani, Opt. Lett. **34**, 3020 (2009).
[26] S. Skupin, R. Nuter, and L. Bergé, Phys. Rev. A **74**, 043813 (2006).
[27] A. Couairon, L. Sudrie, M. Franco, B. Prade, and A. Mysyrowicz, Phys. Rev. B **71**, 125435 (2005).
[28] L. Bergé, S. Skupin, R. Nuter, J. Kasparian, and J.-P. Wolf,

Rep. Prog. Phys. **70**, 1633 (2007).
[29] A. Couairon and A. Mysyrowicz, Phys. Rep. **441**, 47 (2007).
[30] M. Chalfie, Y. Tu, G. Euskirchen, M. W. Ward, and D. C. Prasher, Science **263**, 802 (1994).
[31] R. Heim, D. C. Prasher, and R. Y. Tsien, Proc. Natl. Acad. Sci. U.S.A. **91**, 12501 (1994).
[32] R. Heim, A. B. Cubitt, and R. Y. Tsien, Nature (London) **373**, 663 (1995).
[33] C. Xu, W. Zipfel, J. B. Shear, R. W. Williams, and W. W. Webb, Proc. Natl. Acad. Sci. U.S.A. **93**, 10763 (1996).
[34] B. Boudaïffa, P. Cluotier, D. Hunting, M. A. Huels, and L. Sanche, Science **287**, 1658 (2000).
[35] E. Yablonovitch and N. Bloembergen, Phys. Rev. Lett. **29**, 907 (1972).